Model Development for the Wideband Vehicle-to-vehicle 2.4 GHz Channel

Guillermo Acosta and Mary Ann Ingram

School of ECE, Georgia Institute of Technology,
Atlanta, GA 30332-0250, USA

gte437k@mail.gatech.edu, mai@ece.gatech.edu

Abstract—Statistical channel models are presented for a frequency selective vehicle-to-vehicle or mobile-to-mobile wireless communications link in an expressway environment in Atlanta, Georgia, where both vehicles travel in the same direction. The models were developed from measurements taken using the direct sequence spread spectrum (DSSS) technique at 2.45 GHz. The models imply a non-separable channel with a persistent Rician behavior across multiple model taps.

Model Development for the Wideband Vehicle-to-vehicle 2.4 GHz Channel

Guillermo Acosta and Mary Ann Ingram

School of ECE, Georgia Institute of Technology,
Atlanta, GA 30332-0250, USA

gte437k@mail.gatech.edu, mai@ece.gatech.edu

Abstract—Statistical channel models are presented for a frequency selective vehicle-to-vehicle or mobile-to-mobile wireless communications link in an expressway environment in Atlanta, Georgia, where both vehicles travel in the same direction. The models were developed from measurements taken using the direct sequence spread spectrum (DSSS) technique at 2.45 GHz. The models imply a non-separable channel with a persistent Rician behavior across multiple model taps.

Key words: high mobility channel, per-tap spectra, DSRC, wideband RF channel modeling, time-selective channel.

1. INTRODUCTION

A standard has been developed for vehicle-to-vehicle (VTV) high-speed data communications in the 5.9-GHz Intelligent Transportation Systems Radio Service (ITS-RS) Band. This dedicated short range communications (DSRC) standard [1] defines a short to medium range service, which supports both public safety and private operations in roadside-to-vehicle and VTV communication environments. Examples of VTV applications include warnings for approaching emergency vehicles, impending intersection collisions, and road hazards. This paper applies the method of Mohr et al [2] to extract statistical models from measurements obtained from the expressway site of a VTV channel sounding campaign performed at 2.4 GHz in support of the VTV part of the standards development.

Related works include theoretical 2-D [3] and 3-D [4] double-mobility models, flat-fading VTV measurements for the highway [5], and per-tap Doppler spectra for the fixed-to-vehicle channel [6]. Some examples of long and short term per-tap Doppler spectra for the VTV channel were presented by the authors in [7]; to the author's best knowledge, these were the first reported per-tap VTV channel measured spectra. In this paper, we use an existing model extraction approach to determine an appropriate model for the expressway channel.

The authors gratefully acknowledge the support for this work provided by the National Science Foundation under Grant No. CCR-0121565, and by ARINC, Inc., Contract No. DTFH6199-C-00018.

2. MODEL DEVELOPMENT

In this section, we start by describing the statistical procedure to obtain the parameters describing the model. We then present the obtained models, and we evaluate them by comparing the synthesized model obtained from the statistical analysis with the actual recorded channel.

2.1. Methodology

The channel is measured using the spread spectrum approach described in [3]. The recorded channel is sampled every $\Delta t = 1/B =$ 50 ns, where B is the measurement bandwidth of 20 MHz. The first step in extracting the model is to separate the fast from the slow fading characteristics. We can obtain the slow fading by obtaining the local average power [7]. For this, we require uncorrelated samples of the impulse response (IR) over an appropriate distance that will average out the short-term fading and will not smooth out the long-term fading. This length is usually in the range of 20 to 40 wavelengths, and a sampling at 0.8 ? is usually enough to achieve uncorrelated samples. We calculate the power delay profile (PDP) by averaging the magnitude squared of the IR over the distance

$$P(n\Delta t) = \frac{1}{Q}\sum_{k=0}^{Q-1}\left|h_{norm}\left(n\Delta t, k\Delta t\right)\right|^2 \qquad 0 \le n \le N-1 \quad (1)$$

where $k\Delta t$ is the fixed observation instant of the k-th single IR, Q is the total number of IRs, and h_{norm} indicates short-term fading only. Next, we determine the significant part of the PDP by discarding all parts that are more than 35 dB down from the strongest path.

Let L be the length of the significant part of the PDP divided by Δt . Let M be the number of taps in the model, such that M < L. The L samples are divided into M groups. If the result $L / M = I$ is not an integer, samples with zero amplitude are added to the end of the

PDP. The tapped delay value in each group is found by [2]

$$t_m = \frac{\sum_{n=i_m}^{i_m+I-1} n\Delta t \cdot P(n\Delta t)}{\sum_{n=i_m}^{i_m+I-1} P(n\Delta t)} \quad \text{for} \quad 0 \le m \le M-1 \quad (2)$$

where i_m is the sample number at the start of each group. The delay of the first tap is $t_0 = 0$. Knowing the delay position of the tap, we can obtain the tap magnitude as follows:

$$h_m(t_m, k\Delta t) = \frac{1}{I}\sum_{n=i_m}^{i_m+I-1} h_{norm}(n\Delta t, k\Delta t). \quad (3)$$

So we get K complex tap amplitude values for each tap with delay t_m. The mean amplitude corresponding to each t_m is the average value of the Q amplitude values.

We determine the Rice factor for each tap using the moment-method [9], [10] as follows:

$$\begin{aligned} G_v &= \sqrt{\frac{1}{Q}\sum_{k=1}^{Q}\left(\left|h_m(t_m, k\Delta t)\right|_{k=1}^{k=Q}\right|^2 - \frac{1}{Q}\sum_{k=1}^{Q} h_m(t_m, k\Delta t)\Bigg)^2} \\ |V|^2 &= \sqrt{\frac{1}{Q}\sum_{k=1}^{Q} h_m(t_m, k\Delta t)^2 - G_v^2} \\ K_{Rice} &= \frac{|V|^2}{\frac{1}{Q}\sum_{k=1}^{Q} h_m(t_m, k\Delta t) - |V|^2}. \end{aligned} \quad (4)$$

Finally, we use the Welch algorithm to estimate the Doppler spectrum per tap.

2.2. Resulting Tap Characteristics

For the expressway location, we recorded 14 ten-second takes. We divided each take into 12 0.7-second segments for their analysis. Please note that each take corresponds to a physically different time and location, i.e., each take could be minutes and kilometers apart from another. In Figure 1, we show the PDPs computed for all the 0.7 s segments of the 14 takes. We observe that most of the PDPs die out before 1 μs, because of the generally confined nature of the channel.

Assuming that most commercial channel emulators are six or 12 taps per channel, we decided to generate six and 12-tap channel models. First, we generated a model for each of the 0.7 s segments, and then, we generated overall models. We present the 6 and 12-tap scattering functions for the overall models in Figure 2 and Figure 3, respectively. The corresponding statistical parameters are given in Table 1. The first thing we notice in the Doppler spectra is the "LOS-like" or Rician behavior for each of the first paths. This suggests that there are many reflectors traveling at a similar speed inside a 45 m locus of an ellipse defined by the reflecting path length. We also notice a widening of the Doppler spectra for the later taps. This widening is in accordance to the results of [5]. In several of these later spectra, we can notice some small spikes on the sides of the spectra. These spikes were likely caused by transient paths reflecting from highway overpasses.

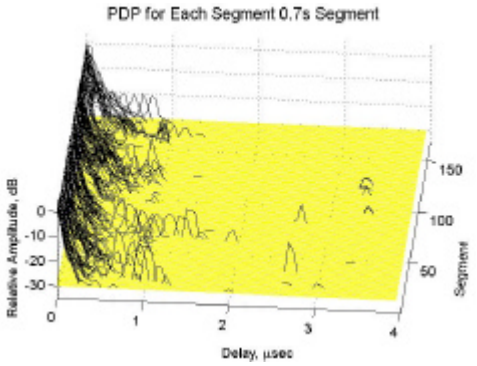

Figure 1: Expressway PDPs

Table 1: 6 and 12 tap model results

Tap	Delay, ns		Magnitude, dB		K_{Rice}	
1	59	53	0.0	0.0	93.4	100.9
2	174	117	-12.0	-7.6	1.1	5.7
3	285	178	-18.3	-14.9	1.3	4.3
4	436	242	-22.5	-18.6	1.7	3.5
5	667	304	-23.3	-21.0	1.1	1.9
6	1050	393	-25.3	-23.8	0.4	0.7
7		530		-25.8		0.3
8		600		-25.4		0.4
9		719		-24.4		0.0
10		842		-24.3		0.1
11		1207		-25.8		0.1
12		1552		-27.6		0.1

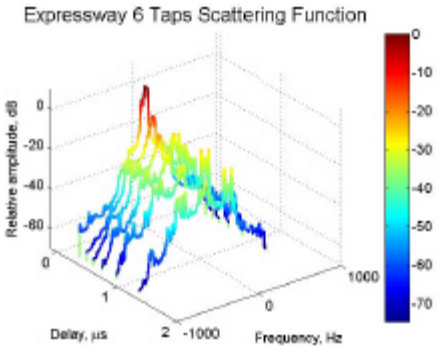

Figure 2: 6 tap model scattering function

We can synthesize the channel using filtered noise on each tap, where the filter characteristics match the spectra of the statistical model [11]. As an example, the estimated scattering function of the synthesized 12 tap

model is shown in Figure 4, which represents a long-time (i.e., 0.7 s) estimation. To confirm the short-time behavior, we estimated the long-term and short-term Doppler spectra of similar taps of the recorded and synthesized channel. For the long-time spectrum, we used the approximately 27,000 IRs in 0.7 s for the estimate, and for the short-time spectra, we obtained the estimate every 2,048 IRs or approximately every 50 ns. In Figure 5, we show the resulting Doppler spectra for the third tap of the synthesized model. In Figure 6, we present the results of a latter tap of one 0.7-second segment of one of the takes of the recorded channel. As we can see in these figures, the short-time spectra of the synthesized channel have transient behavior similar to that of the real channel.

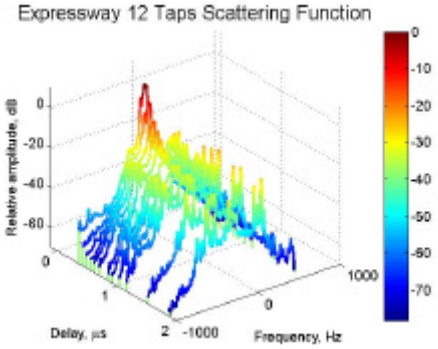

Figure 3: 12 tap model scattering function

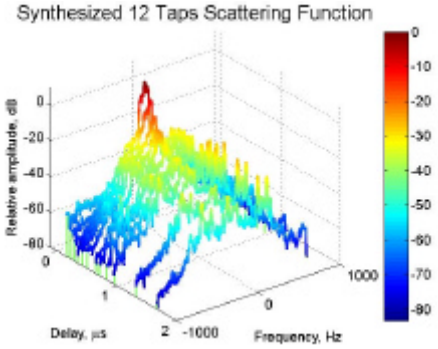

Figure 4: Synthesized 12 tap model scattering function

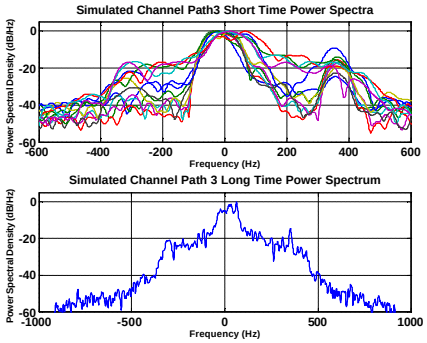

Figure 5: Simulated short time Doppler spectra and long time Doppler spectrum for the third tap of the 12 tap model scattering function

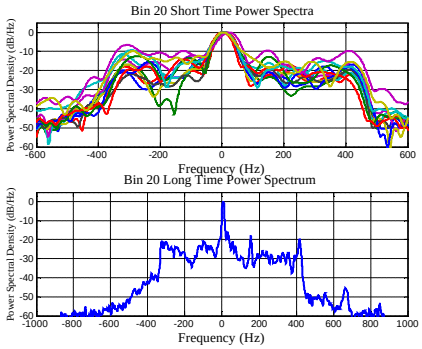

Figure 6: Measured short time Doppler spectra and long time Doppler spectrum of a latter tap of one of the resulting scattering functions

3. Testing Using a DSRC Simulink™ Model

To validate the statistical channel model, we compared the bit error rate (BER) performance of a DSRC link over the recorded channel and over the synthesized channel. We normalized all the channels so that their PDPs had unit area; this includes separate normalization for each measured segment. We developed a Simulink™ model that follows faithfully the specifications of the DSRC standard [1] shown in Table 2. The model includes all the transmission modes and coding. We designed the receiver to include frequency offset compensation based on the algorithm described in [12], and channel adaptive equalization using the pilot tones following the specifications in [13]. The model also contains a signal-to-noise ratio (SNR) threshold detector to adaptively change among the eight transmission modes. The noise is defined as the mean square of the difference between the received complex symbol and its corresponding constellation point. The OFDM symbol is modulated in only 52 subcarriers out of 64 and has 8.0 μs duration with a 1.6

µs guard band interval. The total occupied bandwidth is 8.3 MHz. No thermal noise was added in our simulations.

Table 2: DSRC standard specifications

Data Rate, Mbps	Modulation	Coding Rate	Coded Bits per OFDM Symbol	SNR Threshold dB
3	BPSK	1/2	48	<10
4.5	BPSK	3/4	48	10
6	QPSK	1/2	96	11
9	QPSK	3/4	96	14
12	16-QAM	1/2	192	18
18	16-QAM	3/4	192	22
24	64-QAM	2/3	288	26
27	64-QAM	3/4	288	28

3.1. Results

For the model validation procedure, we performed five different experiments or processes: recorded channel, 12 tap overall model, 12 tap model for each 0.7 s segment, 6 tap overall model, and 6 tap model for each 0.7 s segment. We matched the length of these projects to that of the recorded channel.

For the recorded channel, we have 168 (14 takes x 12 files) 0.7 s segments that we further divided in 0.3 s segments (because of memory limitations) for a total of 336 runs or simulations. Each 0.3 s segment contained 12,000 IRs. For the simulation, we used 68 OFDM symbol frames, four of which were training symbols. Each 0.3 s segment contained 564 frames, and the total number of frames per process was 189,370. For the overall 6 and 12 tap model processes, we used the scattering functions of Figure 2 and Figure 3 as the filter templates for 168 0.7 s different random sequences that produced 4,032,000 different IRs for each process. For the 6 and 12 tap per segment processes, we obtained a scattering function for each 0.7 s segments, producing 168 different models. We then used these 336 to filter another set of 336 0.7 s random sequences. The adaptive modulation system of the model worked in a frame by frame basis. We recorded the BER, SNR, bit rate, and mode for each frame of each process.

In Figure 7 and Figure 8, we show the BER histogram for each of the five processes in terms of 0.3 s segments and in a frame by frame basis. In Figure 9, we present the results for the bit rate in a frame by frame measure. This last figure provides the same information as if we were to present the results using either the SNR or mode. By just looking at the BER results, you might conclude that the 12 tap per segment model is the closest to the recorded channel, but by looking at the bit rate results, we see that the closest is the 12 tap model. We can obtain a better conclusion by measuring the overall BER (i.e., total errors divided by total number of bits transmitted in the 189,370 frames) for each process as shown in Table 3. Here we can see that the best match is the 12 tap model.

Another important result of the channel sounding campaign is the worst case channel. In Figure 10, we present the PDP of the 0.3 s segment with the highest BER of 0.156. We also provide its scattering function in Figure 11. We observe that there are some spikes in the PDP corresponding to excess delays of close to 2 µs and beyond 3 µs. Even though the heights of these spikes are more than 30 dB down from the maximum value of the PDP, they correspond to excess delay values greater than 1.6 µs (the length of the cyclic prefix), and therefore they introduce intersymbol interference, which is particularly harmful to an OFDM receiver. We can also notice a faster widening of the Doppler spectra with many spikes throughout the spectral bandwidth.

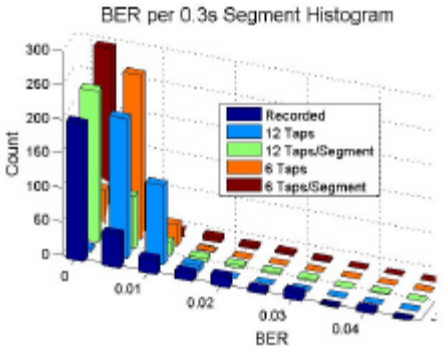

Figure 7: Histogram of the bit error rate for each processed 0.3 s segment

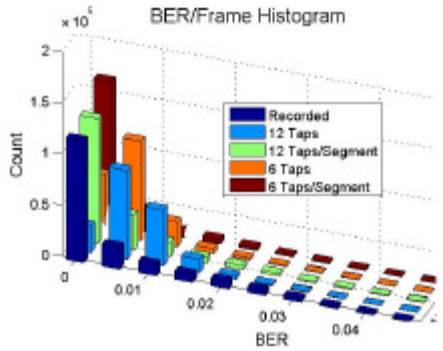

Figure 8: Histogram of the bit error rate for each processed frame

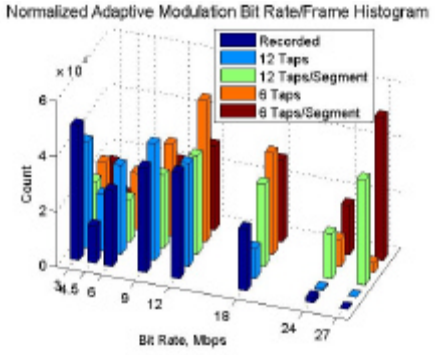

Figure 9: Histogram of the bit rate of each processed frame

Table 3: Final bit error rate for each process

	Bit Error Rate
Recorded Channel	9.76e-3
6 Tap Overall Model	6.83e-3
6 Tap Model for Each 0.7 s Segment	4.16e-3
12 Tap Overall Model	9.56e-3
12 Tap Model for Each 0.7 s Segment	5.32e-3

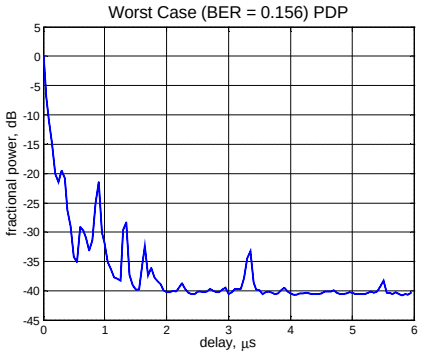

Figure 10: Worst case PDP for a BER = 0.156

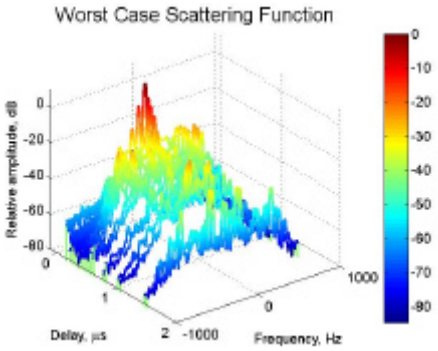

Figure 11: Worst case (BER = 0.156) scattering function

4. CONCLUSIONS

A new 12 tap statistical model has been developed for the V2V frequency selective highway channel when both vehicles travel in the same direction. It has the novel feature of a significant Rician component in first taps. The model was validated in terms of a BER measured compared to the actual recorded channel using a complete DSRC simulation tool.

REFERENCES

[1] ASTM E2213-03, "Standard Specification for Telecommunications and Information Exchange Between Roadside and Vehicle Systems — 5 GHz Band Dedicated Short Range Communications (DSRC) Medium Access Control (MAC) and Physical Layer (PHY) Specifications," ASTM International, www.astm.org,

[2] W. Mohr, "Modeling of wideband mobile radio channels based on propagation measurements," in *Proc. 16th Int. Symp. Personal, Indoor, Mobile Radio Communications*, vol. 2, pp. 397-401, 1995.

[3] C. S. Patel, G. L. Stüber, and T. G. Pratt, "Simulation of Rayleigh faded mobile-to-mobile communication channels," in *Proc. of IEEE Vehicular Technology Conf*., vol.1, pp. 163-167, October 2003.

[4] F. Vatalaro and A. Forcella, "Doppler spectrum in mobile-to-mobile communications in the presence of three-dimensional multipath scattering," *IEEE Trans. on Vehic. Tech.*, vol. 46, no. 1, pp. 213-219, 1997.

[5] J. Maurer, T. Fügenm and W. Wiesbeck, "Narrow-band measurement and analysis of the inter-vehicle transmission channel at 5.2 GHz," in *Proc. of IEEE Vehicular Technology Conf.*, vol. 3, pp. 1274-1278, 2002.

[6] X. Zhao, J. Kivinen, P. Vainikainen, and K. Skog, "Characterization of Doppler spectra for mobile communications at 5.3 GHz," *IEEE Trans. Vehicular Technology*, vol. 52, no. 1, pp. 14-23, 2003.

[7] G. Acosta, K. Tokuda, and M. A. Ingram, "Measured joint Doppler-delay power profiles for vehicle-to-vehicle communications at 2.4 GHz," in *Proc. of IEEE Global Telecom. Conf*., vol. 6, pp. 3813-3817, 2004.

[8] W. C. Y. Lee, "Estimate of local average power of mobile radio signal," in *IEEE Transactions on Vehicular Technology*, vol. 34, No. 1, pp. 22-27, February 1985.

[9] A. Abdi, C. Tepedelenlioglu, M. Kaveh, and G. Giannakis, "On the estimation of the *K* parameter for the Rice fading distribution," in *IEEE Communications Letters*, vol. 5, No. 3, pp. 92-94, March 2001.

[10] L. J. Greenstein, D. G. Michelson, and V. Erceg, "Moment-method estimation of the Ricean *K*-factor," in *IEEE Communications Letters*, vol. 3, No. 6, pp. 175-176, June 1999.

[11] M. C. Jeruchim, P. Balaban, and K. S. Shanmugan, Simulation of Communication Systems: Modeling, Methodology, and Techniques, Second Edition, Kluwer Academic Press, Boston 2000.

[12] J. J. van de Beek, M. Sandell, and P. O. Borjesson, “ML estimation of time and frequency offset in OFDM systems,” in IEEE Transactions on Signal Processing, vol. 45, pp. 1800-1805, July 1997

[13] M. H. Hsieh and C. H. Wei, “Channel estimation for OFDM systems based on comb-type pilot arrangement in frequency selective channels,” in IEEE Transactions on Consumer Electronics, vol. 44, No. 1, pp. 217-225, February 1998.